ELSEVIER

Journal of Power Sources 62 (1996) 51–57

JOURNAL OF POWER SOURCES

Role of minor alloying elements on the performance of lead/acid battery grids. Part 2. Corrosion of lead–arsenic alloys

A.G. Gad Allah [a,*], H.A. Abd El-Rahman [a], M. Abd El-Galil [b]

[a] *Department of Chemistry, Faculty of Science, Cairo University, Giza, Egypt*

[b] *Chloride, Egypt Company for Batteries, Giza, Egypt*

Received 28 July 1995; revised 25 January 1996; accepted 9 February 1996

Abstract

Corrosion of Pb–As alloys (As = 0.1, 0.2, 0.3 and 0.4%) in 5.0 M H_2SO_4 solutions at 30 °C was studied under open-circuit, potentiostatic and galvanostatic polarization conditions. The sulfation process under open-circuit conditions increased as the As concentration increased and the open-circuit potential shifted to more cathodic values. The presence of As affected significantly the potentiostatic polarization curve and caused a substantial decrease in passivity current and increased the overpotentials of both the O_2- and the H_2-evolution reactions. The self-discharging process decreased as the concentration of As increased with formation of substantial amounts of lead oxide beside $PbSO_4$. When Pb–As alloys were subjected to alternative cathodic and anodic galvanostatic polarization cycles, the corrodable layer thickness increased in the order of: Pb–0.1%As > Pb–0.3%As% > Pb–0.4%As > Pb > Pb–0.2%As. The efficiency of PbO_2 formation also depended on the percentage As.

Keywords: Lead/acid batteries; Arsenic; Corrosion

1. Introduction

Antimonial lead alloys containing low antimony, ≃0.2% As and/or Sn [1–6] and sometimes <0.1% Se [7–9] were developed for the manufacture of superior grids in lead/acid batteries. Low percentages of As are known to increase the hardness and to improve the casting properties of Pb–As alloys [10] but the corrodability was found to increase at As > 0.1% [11]. The role of As on the charging and discharging characteristics, however, has received little attention.

In the present work the corrosion of Pb–As alloys (As = 0.1, 0.2, 0.3 and 0.4%) was studied under open-circuit and polarization conditions in 5.0 M H_2SO_4 solutions at 30 °C. It is aimed to explore the role of As on the corrodability of Pb–As alloys during the charging, discharging and self-discharging processes.

2. Experimental

The disc electrodes used (surface area: 0.196 cm^2) were made from Pb–As alloys cast in the form of cylindrical rods. Spec-pure Pb and As were used for casting by adding a known weight of As to the molten Pb at 500 °C under N_2 atmosphere and the melt was kept at this temperature for 6 h, after which the melt was poured into the cylindrical moulds. The exact amount of As in the alloy was 0.098, 0.190, 0.297 and 0.395 for the alloys Pb–0.1%As, Pb–0.2%As, PbO–0.3%As, and Pb–0.4%As, respectively, determined by atomic absorption spectrophotometry (Perkin-Elmer 2380). The electrodes were mechanically polished with successively finer grades of emery papers down to 4/0, then with alumina powder (0.05 μm), cleaned thoroughly wih a soft tissue, degreased with alcohol and finally rinsed with distilled water.

The sulfuric acid solution used (5.0 M) was prepared from an AnalaR grade concentrated H_2SO_4 solution and triple-distilled water. All potentials were measured and referred to a (Hg/Hg_2SO_4/1.0 M H_2SO_4) reference electrode, E = 0.682 V versus NHE.

The electrolytic cell and a.c. impedance bridge (Wien Type) were described in Ref. [12]. The cell impedance was balanced against a series connection of calibrated variable resistances and capacitances at 1.0 kHz. Steady-potentiostatic polarization curves were recorded with a scanning potentiostat (EG&G Model 362) and a digital multimeter.

* Corresponding author.

0378-7753/96/$15.00 © 1996 Elsevier Science S.A. All rights reserved
PII S0378-7753(96)02398-1

Galvanostatic polarization was made by using an electronic constant current unit and an x–y recorder. All experiments were carried out at 30 ± 0.2 °C.

3. Results and discussion

3.1. Open-circuit behaviour

The currentless open-circuit potential, E_{corr}, capacitance, C_m, and resistance, R_m, for Pb–As alloys containing 0.1, 0.2, 0.3 and 0.4% As in 5.0 M H_2SO_4 solutions at 30 °C were followed with time until steady-state values were attained. As seen in Fig. 1(a), the potential drifts first to less negative values, then to slightly more positive untill a steady state has been reached. The effect of As on the steady-state potential, E_{ss}, is observed in Fig. 1(b). The thermodynamic potentials of the systems $Pb/PbSO_4$ and As/As_2O_3 versus Hg/Hg_2SO_4, 1.0 M H_2SO_4 reference electrode [13] are given by

$$E_{Pb/PbSO_4} = -1.038 - 0.03 \log a_{SO_4^{2-}} \quad (1)$$

and

$$E_{As/As_2O_3} = 0.448 - 0.059pH \quad (2)$$

The value of $a_{SO_4^{2-}}$, 5.0 M H_2SO_4, is equal to 1.58 M [14], and the value of $E_{Pb/PbSO_4} = -1.044$ V versus Hg/Hg_2SO_4, 1.0 M H_2SO_4.The recorded steady-state open-circuit potentials, E_{ss}, for Pb and Pb–As alloys are -1.03 and -1.15 V, respectively. Therefore, the potential observed is close to the reversible potential of the $Pb/PbSO_4$ system and it is a mixed one. Generally, one may look at the presence of microscopic galvanic cells between Pb and As on the electrode where As acts as a centre for the cathodic process. The corrodability

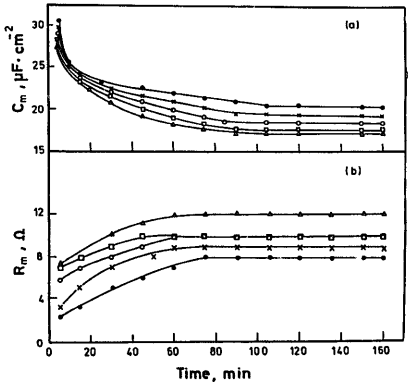

Fig. 2. Electrode impedance components of pure lead and alloys of Pb–As in 5 M H_2SO_4 solutions at 30 °C: (a) capacitance, C_m, and (b) resistance, R_m. (●) Pure lead, (x) Pb–0.1%As, (○) Pb–0.2%As, (□) Pb–0.3%As, and (Δ) Pb–0.4%As.

which is cathodically controlled, increases with increasing As percent, cf. Fig. 1(b).

Fig. 2(a) and (b) shows the variation of the electrode impedance, i.e. C_m and R_m, with time. First the capacitance decreases rapidly, then slowly attains a more or less stabilized value, see Fig. 2(a). On the contrary, the inverse behaviour is observed for R_m, Fig. 2(b). Plots of steady-state capacitance, $(C_m)_{ss}$, and resistance, $(R_m)_{ss}$, versus the percentage As are observed in Fig. 3(a) where the inverse correlation between $(C_m)_{ss}$, and $(R_m)_{ss}$ is clearly demonstrated. The decrease in C_m and the increase in R_m are attributed to formation of the $PbSO_4$ layer. Assuming that the formed layer

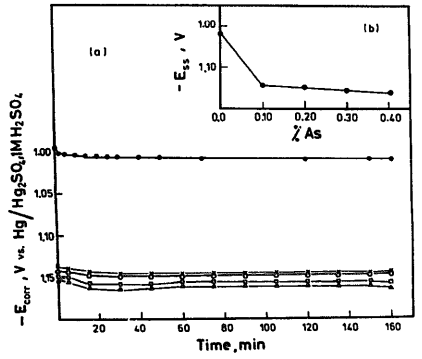

Fig. 1. .a) Variation of corrosion potential of pure lead and alloys of Pb–As electrodes in 5 M H_2SO_4 solutions at 30 °C with time. (●) Pure Pb, (x) Pb–0.1% As, (○) Pb–0.2%As, (□) Pb–0.3%As and (Δ) Pb–0.4%As. b) Plots of steady-state corrosion potential vs. percentage As of Pb–As alloys in 5.0 M H_2SO_4 solution at 30 °C.

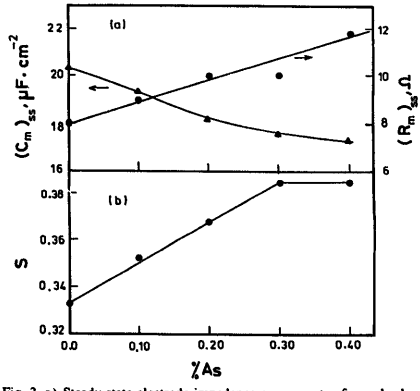

Fig. 3. a) Steady-state electrode impedance components of pure lead and alloys of Pb–As in 5 M H_2SO_4 solutions at 30 °C vs. percentage As: a(▲) capacitance, $(C_m)_{ss}$, and (●) resistance, $(R_m)_{ss}$. (b) Surface coverage, S, vs. percentage As.

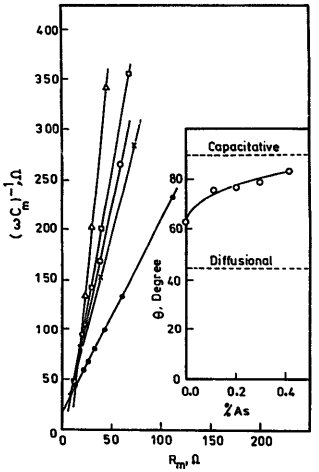

Fig. 4. Electrode impedance of pure lead and alloys of Pb–As in complex plane. (●) Pure Pb, (x) Pb–0.1%As, (○) Pb–0.2%As, (□) Pb–0.3%As and (Δ) Pb–0.4%As. Inset: phase shift, θ, vs. percentage As.

is described in terms of C_m, the surface coverage, S, is calculated using the following equation

$$S=\frac{(C_m)_0-(C_m)_{ss}}{(C_m)_0} \quad (3)$$

where $(C_m)_0$ and $(C_m)_{ss}$ are the initial and steady-state capacitance, respectively. The effect of percentage As on surface coverage is illustrated in Fig. 3(b). It is obvious that the fraction of surface covered by $PbSO_4$ increases with increasing percentage As.

Impedance values, after the steady state was reached, were traced as a function of frequency and are represented in complex plane (Cole–Cole plots) in Fig. 4. For all alloys studied, the impedance, $(\omega C_m)^{-1}$, increases as the frequency decreases within the 200–10 000 Hz range, and it tends to be more capacitative with increasing percentage As. The variations are linear ones. The values of slope, $d(\omega C_m)^{-1}/dR_m$, and phase shift, $\theta=\tan^{-1}$ slope, increases with increasing percentage As while that of the dielectric loss angle, $\delta=90°-\theta$, decreases in the same way. Such data are consistent with increasing the corrodability as the percentage As increases.

3.2. Potentiostatic polarization

Prior to polarization, the electrodes were held at −1.7 V for 30 min to remove any reducible layer on the metal surface. The potential was then increased in the anodic direction in 5–50 mV steps and the respective quasi-steady currents were recorded within 2–10 min for each step. The potential was scanned in the −1.7 to 1.8 V range to cover the electrochemical behaviour of Pb–As alloys from H_2-evolution reaction to O_2-evolution reaction. Fig. 5 shows the potentiostatic anodic polarization curves for Pb–As alloys in 5.0 M H_2SO_4 solutions. Starting from the steady-state open-circuit potential, E_{ss}, the current in region I increased due to the oxidation of Pb to Pb^{2+} almost reversibly [15] until a critical potential, E_c, was obtained about −0.970 V where $PbSO_4$ started to nucleate. In the presence of As, the current decreased thereafter sharply until the passivity current, i_p^{II}, was reached while it starts to increase again to a more or less stable value for Pb. The critical passivation current, i_c (at E_c), was higher than i_p^{II} in the presence of As in contrast to pure Pb. Quite stabilized i_p^{II} values could be observed in the presence of As > 0.1% in the potential range from about −0.90 to 0.2 V, −0.1 to 0.0 V for Pb–0.2%As, Pb–0.3%As, and Pb–0.4%As, respectively (region II). For the alloy Pb–0.1%As the current at $E>E_c$ decreases sharply to $\sim 1.5\times10^{-5}$ A cm^{-2} ($E=-0.900$ V) then started to increase to a more or less stable value $\sim 3.5\times10^{-5}$ A cm^{-2}. The increase in passivity current at $E>-0.60$ V is connected to the growth of PbO under the sulfate layer according to the following reactions (region III) [16,17]

$$4Pb+SO_4^{2-}+4H_2O=3PbO\cdot PbSO_4\cdot H_2O+6H^++8e^- \quad (4)$$

and

$$Pb+H_2O=PbO+2H^++2e^- \quad (5)$$

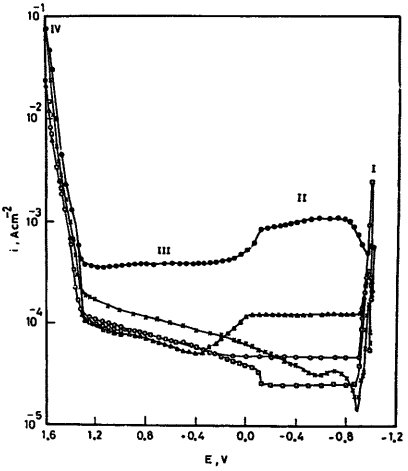

Fig. 5. Potential–log i polarization curves for alloys of Pb–As electrodes in 5.0 M H_2SO_4 solutions at 30 °C. (●) Pure Pb, (x) Pb–0.1%As, (○) Pb–0.2%As, (□) Pb–0.3%As and (Δ) Pb–0.4%As.

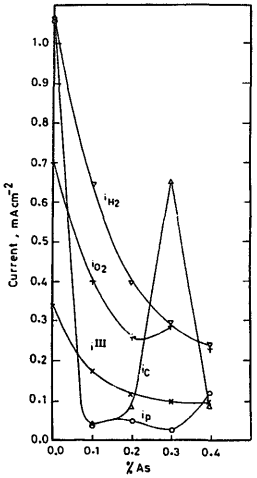

Fig. 6. Dependence of the passivity current (○) i_p^{II}, the current in region III at +1.200V, (x) i^{III}, (+) the O_2-evolution current at +1.500V, i_{O_2}, (▽) the H_2-evolution current at $E = -1.300$V, i_{H_2}, and (△) the critical passivition current i_c, on percentage As.

The reversible potentials for the redox processes (4) and (5) in 5.0 M H_2SO_4 solutions at 30 °C is −0.652 and −0.434 V, respectively. For the alloys containing As > 0.1%, the formation of PbO seems to be inhibited to varying extents depending on the percentage As until the condition of the PbO formation was fulfilled. This condition is caused by the decrease in acidity of the environment under the $PbSO_4$ layer, blocking the diffusion of H_2SO_4 through the more or less protective $PbSO_4$ layer. The protection of the $PbSO_4$ layer increases in the order Pb–0.4%As < Pb–0.2%As < Pb–0.3%As. Thus the current even decreases as a result of PbO formation in the case of Pb–0.4%As. At $E \geq 0.30$ V, the current shows a little dependence on the percentage As. Fig. 6 shows the dependence of some electrochemical parameters on the percentage As. Generally, all currents decreased in the presence of As regardless of its percent. The minimum i_p^{II} was recorded for Pb–0.3%As and also the maximum i_c among the Pb–As alloys. The current in the region of PbO and $PbSO_4$ growth (region III), i^{III}, decreased with the increasing concentration of As. The current in O_2-evolution (regicn IV) decreased in the order: Pb > Pb − 0.1%As > Pb − 0.3% As > Pb − 0.2%As > Pb − 0.4%As whereas the current in the H_2-evolution region decreases as the percentage As increases.

3.3. Galvanostatic polarization

The electrodes were cathodically polarized at 510 μA cm^{-2} for 30 min to obtain the steady-state potential corresponding to the H_2-evolution. Then the polarity was reversed in the anodic direction and the potential–time curve was recorded for 30 min before reversing the polarity again to discharge the electrodes until the potential was reached before

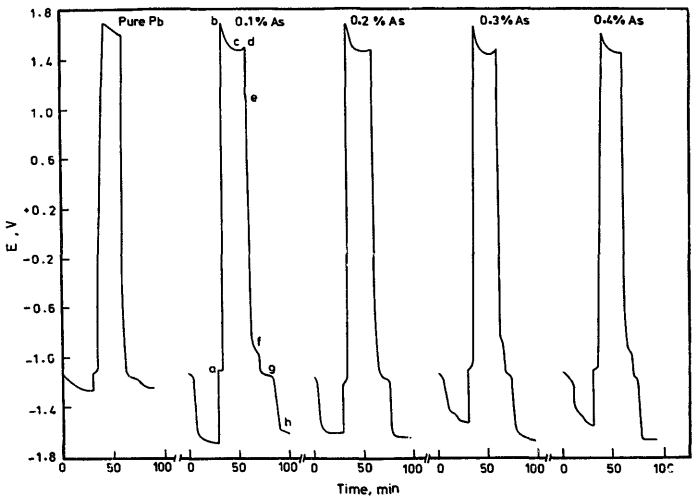

Fig. 7. Cyclic galvanostatic polarization curves for Pb and Pb–As alloys in 5.0 M H_2SO_4 solution at 30 °C. The current density = 510 μA cm^{-2}.

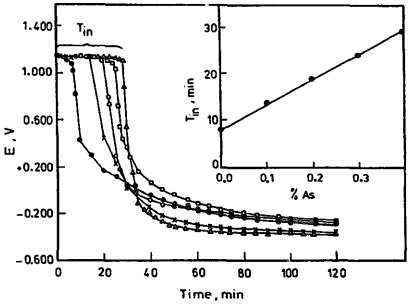

Fig. 8. The potential decay curves for self-discharge of Pb–As alloys after 1 h charging at a constant current density of 510 μA cm^{-2} in 5.0 M H_2SO_4 solution at 30 °C vs. time. (●) Pure Pb, (x) Pb–0.1%As, (○) Pb–0.2%As, (□) Pb–0.3%As and (Δ) Pb–0.4%As. Inset: induction time, T_{in}, vs. percentage As.

charging commenced Fig. 7. Generally, the main features of these curves can be summarized as follows [16–18]

1. formation of $PbSO_4$ at $\simeq -1.0$ V (arrest a)
2. formation of PbO_2 (maximum b)
3. transformation of $PbSO_4$ into PbO_2 (minimum c)
4. O_2-evolution (maximum d)
5. reduction of PbO_2 into Pb^{II} (arrest e)
6. reduction of basic sulfate into Pb metal (arrest f)
7. reduction of $PbSO_4$ into the metal (arrest g)
8. H_2-evolution (arrest h)

Also, it is noticed that no additional arrests due to the presence of As could be observed and the variation of the percentage As had a little effect on the arrest potentials. The arrest due to the discharge of PbO_2 into $PbSO_4$ at $\simeq 1.14$ V is clearly demonstrated after a longer charging period at 510 μA cm^{-2} for 1 h during the open-circuit potential decay as can be seen in Fig. 8. An induction period at $\simeq 1.14$ V appeared before the rapid decay of potential to quasi-steady value $\simeq -0.4$ V, the time of the induction period, T_{in}, before the decay increases as the percentag As increases. The induction period is attributed to the transformation of PbO_2 into $PbSO_4$ through a self-discharging process. In this process, PbO_2 is reduced into $PbSO_4$ while the underlying Pb is oxidized into $PbSO_4$. PbO_2 could also be reduced at the expense of other processes, e.g. O_2-evolution and H_2-oxidation [19,20]. The self-discharging process is accompanied by substantial changes in the capacitance and resistance as can be seen in Fig. 9. The increase in R_m and the decrease in C_m with time is attributed to the transformation of the conducting PbO_2 into the insulating $PbSO_4$ and PbO [20,21]. The insulating properties after self-discharging increases in the order: Pb − 0.4%As < Pb − 0.2%As < Pb − 0.3%As which is the same order reported in the potentiostatic polarization curves at the quasi-steady potential after decay $\simeq -0.40$ V, see Fig. 5. Generally, the presence of As decreases the rate of self-sulfation.

The total cathodic charge, Q_{ca} was determined by multiplying the time until the onset of the H_2-evolution reaction by the discharging current density. Q_{ca} is related to the electrochemical processes occurring during discharge process through the equation

$$Q_{ca} = Q^r_{PbO_2 \rightarrow Pb^{2+}} + Q^r_{PbO \cdot PbSO_4} + Q^r_{PbSO_4} \quad (6)$$

where the superscript 'r' refers to reduction and subscripts refer to the species to be reduced. Side reactions such as O_2-reduction were neglected. Due to the self-discharging process, $Q^r_{PbO_2 \rightarrow Pb^{2+}}$ was found to be much lower than $(Q^r_{PbO \cdot PbSO_4} + Q^r_{PbSO_4})$. The charge would be consumed in reduction of PbO_2 if the self-discharging process was absent, Q_{sd}, could be estimated approximately as follows

$$Q_{sd} = 1/2(Q^r_{PbO \cdot PbSO_4} + Q^r_{PbSO_4}) - Q^r_{PbO_2 \rightarrow Pb^{2+}} \quad (7)$$

The above equation implies that the self-discharging occurred only through the oxidation of the underlying Pb and other processes were discounted. Thus the actual amount of

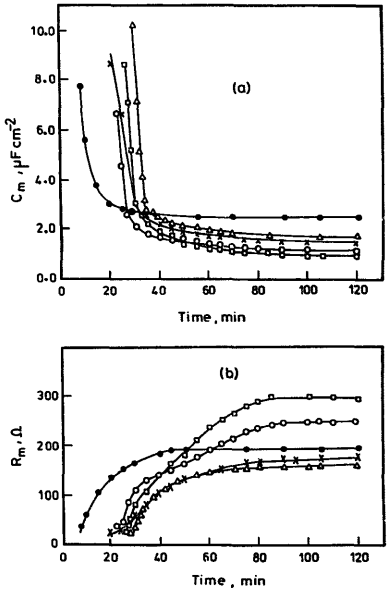

Fig. 9. (a) Variation of capacitance, C_m, and (b) resistance, R_m, during the self-discharge of Pb–As alloys in 5.0 M H_2SO_4 solution at 30 °C with time. (●) Pure Pb, (x) Pb–0.1%As, (○) Pb–0.2%As, (□) Pb–0.3%As and (Δ) Pb–0.4%As. The electrodes were charged at a current density of 510 μA cm^{-2} for 1 h before the self-discharge process.

charge involved in the reduction of PbO_2 into Pb^{2+} is given by

$$Q^{total}_{PbO_2 \rightarrow Pb^{2+}} = Q^{r}_{PbO_2 \rightarrow Pb^{2+}} + Q_{sd} \quad (8)$$

On the other hand, the total anodic charge, Q_{an}, is consumed in the following processes

$$Q_{an} = Q^{f}_{PbSO_4} + Q^{f}_{Pb \rightarrow PbO_2} + Q^{f}_{PbSO_4 \rightarrow PbO_2} + Q^{f}_{O_2} \quad (9)$$

where the superscript 'f' refers to formation of the compounds given as subscripts. The charge consumed in the reduction of PbO_2 to Pb, $Q^{total}_{PbO_2 \rightarrow Pb}$, is given by multiplying the right-hand side of Eq. (8) times two. The total charge consumed in the formation of PbO_2 from Pb, $Q^{total}_{PbO_2 \rightarrow Pb}$, according to Eq. (9) is given by

$$Q^{total}_{Pb \rightarrow PbO_2} = Q_{an} - Q^{f}_{O_2} \quad (10)$$

The charge balance implies that $Q^{total}_{Pb \rightarrow PbO_2}$ equals in magnitude and opposite in sign to $Q^{total}_{Pb \rightarrow PbO_2}$ and so the efficiency of PbO_2 formation during the charging process, $f^{r}_{PbO_2}$, could simply be estimated from the relation

$$f^{r}_{PbO_2} = (Q^{r}_{PbO \cdot PbSO_4} + Q^{r}_{PbSO_4}) / Q_{an} \quad (11)$$

All the quantities on the right-hand side of Eq. (11) can be determined from the cyclic galvanostatic polarization curves, cf. Fig. 7. $f^{r}_{PbO_2}$ as a function of the percentage As is given in Table 1. As can be seen, the oxide formation efficiency increases in the order: Pb − 0.3%As < Pb − 0.2%As = Pb − 0.4%As < Pb < Pb − 0.1As.

3.4. Effect of charging–discharging cycles

The electrodes were subjected to alternative cathodic and anodic cycles at a current density of 5.1 mA cm^{-2} (half-cycle time: 10 min) and were discharged at 0.255 mA cm^{-2} after several polarization cycles, N. At the end of the discharge, the polarity was reversed in the anodic direction and the amount of charge corresponding to $PbSO_4$ formation was determined. Figs. 10-12 show the dependence of the total cathodic charge, Q_{ca}, the charges consumed in reduction of basic lead sulfate, $Q^{r}_{PbO \cdot PbSO_4}$, and lead sulfate, $Q^{r}_{PbSO_4}$, and the charge consumed in formation of lead sulfate, $Q^{f}_{PbSO_4}$, on the number of galvanostatic polarization cycles. The polarization program is shown in the bottom part of Fig. 10. The following conclusions can be drawn from Figs. 10–12:

(i) Q_{ca} for Pb is higher than for Pb–As alloys but it increases generally with increasing N, especially for the alloys Pb–0.2%As, cf. Fig. 10. The increase in Q_{ca} with N indicates a deepening of the surface layer subjected to self-discharging. As N increases, new underlying Pb layers were involved in the self-discharging process and at the end of the complete discharging to the onset of H_2-evolution, thicker spongy Pb layers were obtained. The results showed that Pb was relatively more resistive than Pb–As alloys for this process and Pb–0.2%As showed the highest increase. At a value N > 10, it may be expected that Q_{ca} values for Pb–As alloys

Table 1
Charges consumed in the reduction of $PbO_2 \rightarrow Pb^{2+}$, basic lead sulfate, and lead sulfate and the efficiency of PbO_2 formation. The current density used in charging and discharging was 510 $\mu A\ cm^{-2}$ and temperature 30 °C. The electrolyte was 5.0 M H_2SO_4

Alloy	$Q^{r}_{PbO_2 \rightarrow Pb^{2+}}$ (C cm^{-2})	$Q^{r}_{PbO \cdot PbSO_4}$ (C cm^{-2})	$Q^{r}_{PbSO_4}$ (C cm^{-2})	$f^{r}_{PbO_2}$ [a]
Pb–0.0%As	0.008	0.092	0.519	0.68
Pb–0.1%As	0.031	0.367	0.367	0.86
Pb–0.2%As	0.015	0.153	0.367	0.59
Pb–0.3%As	0.015	0.153	0.336	0.56
Pb–0.4%As	0.015	0.244	0.276	0.59

[a] Calculated according to Eq. (11) using $Q_{an} = 0.92$ C cm^{-2}.

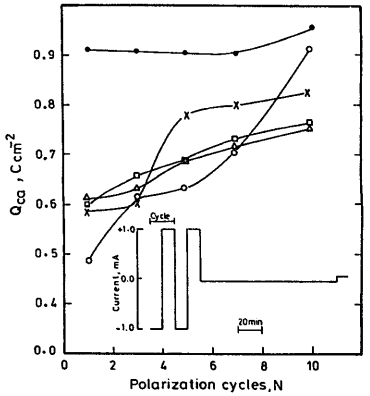

Fig. 10. Dependence of the total cathodic charge, Q_{ca}, on the number of galvanostatic polarization cycles, N, for Pb–As alloys in 5.0 M H_2SO_4 solution at 30 °C. (●) Pure Pb, (x) Pb–0.1%As, (○) Pb–0.2%As, (□) Pb–0.3%As and (Δ) Pb–0.4%As. The galvanostatic polarization program is shown in the lower part of the figure.

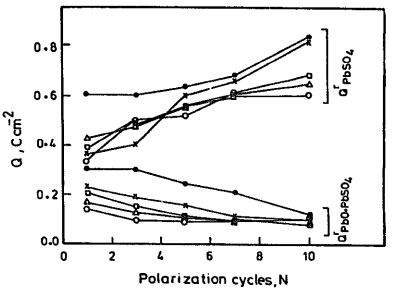

Fig. 11. Dependence of the charges consumed in reduction of basic lead sulfate, $Q^{r}_{PbO \cdot PbSO_4}$, and lead sulfate, $Q^{r}_{PbSO_4}$, on the number of galvanostatic polarization cycles, N, for Pb–As alloys in 5.0 M H_2SO_4 solution at 30 °C. (●) Pure Pb, (x) Pb–0.1%As, (○) Pb–0.2%As, (□) Pb–0.3%As and (Δ) Pb–0.4%As.

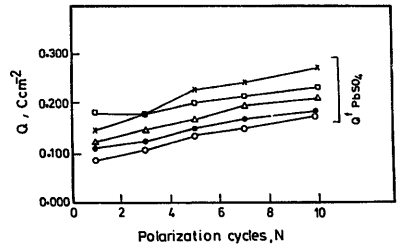

Fig. 12. Dependence of the charge consumed for formation $PbSO_4$, $Q^f_{PbSO_4}$, on the number of galvanostatic polarization cycles, N, for Pb–As alloys in 5.0 M H_2SO_4 solutions at 30 °C. (●) Pure Pb, (x) Pb–0.1%As, (○) Pb–0.2%As, (□) Pb–0.3%As and (Δ) Pb–0.4%As.

approach that of Pb or even exceed it, especially Pb–0.2%As. Thus, Pb–As alloys suffered from higher corrodability than Pb as the number of polarization cycles increases.

(ii) Generally, $Q^r_{PbO\cdot PbSO_4}$ decreases as N increases while $Q^f_{PbSO_4}$ showed the opposite trend and the values of the latter charge are higher than the former, for the same N, cf. Fig. 11. This indicates that the amount of $PbO\cdot PbSO_4$ formed during the discharge of $Pb^{IV} \rightarrow Pb^{II}$ decreased as N increased, probably due to the formation of more opened and porous layers. Thus, the diffusion of the acid through the layers became faster and the condition of PbO formation became more difficult to be achieved. Consequently, the layer was mainly $PbSO_4$ as proved by the increases of $Q^f_{PbSO_4}$ at the expense of $Q^r_{PbO\cdot PbSO_4}$.

(iii) The argument that the thickness of the spongy Pb layer increased with increasing N, is clearly demonstrated in Fig. 12. The amount of charge required to form the insulating $PbSO_4$ layer, $Q^f_{PbSO_4}$ increased as the number of cycles increased. In this respect, the thickness of the spongy Pb layer increased in the order: Pb–0.2%As < Pb < Pb–0.4%As < Pb–0.3%As < Pb–0.1%As.

4. Conclusions

Arsenic affected the electrochemical behaviour of lead in 5.0 M H_2SO_4 solutions. It increases the sulfation process under open-circuit conditions and the corrosion layer is composed of $PbSO_4$. All currents decreased under potentiostatic polarization, generally, in the presence of As regardless of its percentage. The current in O_2- and H_2-evolution regions decreased in the order: Pb > Pb–0.1%As > Pb–0.3%As > Pb–0.2%As > Pb–0.4%As.

Galvanostatic polarization curves showed no additional arrests due to the presence of As and its variation had little effect on the different arrest potentials. An induction period at ≃ 1.14 V appeared before the rapid decay of potential to the quasi-steady value, its length increases as the percentage As increases. On repeating charging and discharging, a thicker spongy layer grew with increasing the number of cycles, the order of its increase is: Pb–0.2%As < Pb < Pb–0.4%As < Pb–0.3%As < Pb–0.1%As.

References

[1] N.A. Novikova, V.P. Dervyagina, I.S. Dankova, N.V. Milovidova, M.H. Dasoyan and A.A. Ravdel, *Zh. Prikl. Khim., 44* (1971) 2447.
[2] W. Zhau and X. Chen, *Huaxue Xuebao, 43* (1985) 33; *44* (1986) 399.
[3] J. Sklarchuk, M.J. Dewar, E.M. Valeriote and A.M. Vincze, *J. Power Sources, 42* (1993) 47.
[4] H. Lin, P. Xu and W. Zhou, *Yengyong Huxue, 8* (1991) 60.
[5] T. Ozako, K. Ootsubo, Y. Sakata and S. Fukuda, *Jpn. Kokai Tokkyo Koho JP Patent No. 02 262 251* (1990).
[6] D. Pavlov, A. Dakhuche and T. Rogachev, *J. Power Sources, 30* (1990) 177.
[7] Y. Huang, *Faming Zhuanli Shenging Gongkaishuoming Shu, CN Patent No. 1 055 204* (1991).
[8] S. Osumi and T. Omae, *Jpn. Kokai Tokkyo Koho, JP Patent No. 04 02 055* (1992).
[9] J. Germy, F. Kalab, J. Miskovsky and M. Matezka, K.F. Varm, J. Miskovsky, M. Malejka and K. Vurm, *Czech. CS. Patent No. 262 883* (1990).
[10] G.W. Vinal, *Storage Batteries*, Wiley, New York, 4th edn., 1962. p. 20.
[11] O. Emicke, *Metall, 4* (1950) 1; 48.
[12] A.G. Gad. Allah, H.A. Abd El-Rahman, S.A. Salih and M. Abd El-Galil, *J. Appl. Electrochem., 22* (1992) 571.
[13] M. Pourbaix, *Atlas of Electrochemical Equilibria in Aqueous Solutions*, NACE, Houston, TX, USA, 1974, p. 485; 516.
[14] H.S. Harned and W.J. Hamer, *J. Am. Chem. Soc., 57* (1935) 27.
[15] L.M. Baugh, K.L. Bladen and F.L. Tye, *J. Electroanal. Chem., 145* (1983) 355.
[16] M.N.C. Ijomah, *J. Electrochem. Soc., 134* (1987) 2960.
[17] Y. Yamamoto, K. Fumino, T. Ueda and M. Nambu, *Electrochim. Acta, 37* (1992) 199.
[18] F.E. Varela, L.M. Gassa and J.R. Vilche, *Electrochim. Acta, 37* (1992) 1119.
[19] K.R. Bullock and E.C. Laird, *J. Electrochem. Soc., 129* (1982) 1393.
[20] V. Iliev and D. Pavlov, *J. Electrochem Soc., 129* (1982) 458.
[21] D. Pavlov and I. Balkamov, *J. Electrochem. Soc., 134* (1987) 2390.